Songklanakarin J. Sci. Technol.
32 (2), 181-187, Mar. - Apr. 2010

Songklanakarin Journal of Science and Technology
http://www.sjst.psu.ac.th

Original Article

Design of a quadratic filter for contrast - assisted ultrasonic imaging based on 2D gaussian filters

Tosaporn Nilmanee* and Pornchai Phukpattaranont

Department of Electrical Engineering, Faculty of Engineering
Prince of Songkla University, Hat Yai, Songkhla, 90112 Thailand.

Received 28 September 2007; Accepted 18 May 2009

Abstract

We present a novel design of quadratic filters (QFs) in the frequency domain in order to improve the quality of contrast-assisted ultrasound images for medical diagnosis. The QF is designed as a 2D linear-phase filter. In addition, the magnitude is based on the sum of two 2D Gaussian filters. The centers of the Gaussian filters are placed at the locations where the power strength of signals from ultrasound contrast agent over surrounding tissue is maximal. The design parameters consist of two centers and a standard deviation (SD) of the Gaussian filters. The coefficients of the QF are obtained using the inverse discrete Fourier transform. The QFs from the proposed design method are evaluated using *in vivo* ultrasound data, i.e., the kidney of a guinea pig. We find that the appropriate SD and two center points of the QF for the *in vivo* data are at 0.34, (3.30, 3.30) and (-3.30, -3.30) MHz, respectively. Results show that the images produced from the output signals of the new design are superior to the original B-mode both in terms of contrast and spatial resolution. The quadratic image provides clear visualization of the kidney shape and large vascular structures inside the kidney. The contrast-to-tissue ratio value of quadratic image is 24.8 dB compared to -1.5 dB from the B-mode image. In addition, we can use this new design approach as an efficient tool to further improve the QF in producing better contrast-assisted ultrasound images for medical diagnostic purposes.

Keywords: ultrasound contrast agents, quadratic filter, volterra filter, quadratic image, ultrasound imaging

1. Introduction

An ultrasound contrast agent (UCA) is an external substance that is usually introduced into the vascular system. Most of current UCAs are in the form of encapsulated microbubbles. Compositions that allow them to traverse the lung capillary beds are the gaseous core with high molecular weights and the stabilized encapsulated shell. Gases with large molecules have low diffusion constants. As a result, their low diffusion rates reduce their dissolvability in fluids, such as blood and water (Feinstein *et al.*, 1984). On the other hand, the encapsulation with lipid or albumin shell prevents inner gases from the swift process of diffusing through the surrounding liquid.

Perfused tissues containing microbubbles provide higher echogenicity than that of normal tissues because of differences in acoustic properties of the surrounding tissue media relative to those with microbubbles. Moreover, at certain levels of excitation, radial oscillations of microbubbles due to compressional and rarefactional cycles of the applied pressure are not symmetrical resulting in harmonic echoes, i.e., the fundamental (f_0) and its higher multiple frequencies ($2f_0$, $3f_0$,...) (De Jong *et al.*, 1994a,b). These harmonic frequencies, especially the second harmonic, are significantly higher than those from the surrounding tissue and can be exploited in the separation of UCA echoes from the surrounding medium. State-of-the-art ultrasonic imaging modalities utilize nonlinear oscillation from UCAs to enhance diagnostic capabilities in medical applications (Frinking, 2000). Consequently, many reports of the improved diagnostic capabilities exploit-

*Corresponding author.
Email address: tj_spy@hotmail.com

ing UCAs in clinical applications have been published (Cosgrove, 2006). Examples include improved discrimination between benign and malignant liver tumors (Ramnarine *et al.*, 2000), improved depiction of the vascularity of cancerous tumors occurring in the liver (Tanaka *et al.*, 1995), and enhanced assessment of myocardial perfusion (Frischke *et al.*, 1997)

We have validated the use of a quadratic filter (QF) for separating the linear and quadratic components of the beamformed radio frequency (RF) data in pulse-echo ultrasonic imaging (Phukpattaranont and Ebbini, 2003). The quadratic component from the QF captures the second order nonlinearities in the echo data, i.e., both the low frequency and the second harmonic. Grayscale images from the quadratic component, referred to as quadratic images, typically have higher contrast and increased dynamic range than the standard B-mode images (without loss in spatial resolution). An algorithm for finding the coefficients of the QF was developed based on a linear plus quadratic prediction model of the RF data in the time domain. In this paper, we propose a new method to design the QF in the frequency domain for separating quadratic components. The new approach not only significantly reduces the computational complexity of the design but also provides the QF with better performance in producing the images for medical diagnosis.

The remainder of this paper is organized as follows: Section 2 provides the details in designing the QF for contrast-assisted ultrasonic imaging based on 2D Gaussian filters Section 3 describes the details of experimental setup, data acquisition, power spectrum computation, and contrast measurement Section 4 gives results and discussion whereas Section 5 draws the conclusions.

2. Quadratic Filter Design

In Phukpattaranont and Chetpattananondh (2005) we analyze the characteristics of the QF designed with a linear plus quadratic prediction model in the frequency domain. It has been shown that the appropriate property of the QF for separating quadratic components from UCA is to have a passband in the 2D frequency domain where the contrast-to-tissue ratio of UCA over surrounding tissue is maximal. Consequently, we utilize this ratio as a reference to design the QF in the frequency domain for separating UCA signals from tissue echoes. The linear-phased QF is designed based on the sum of two 2D Gaussian filters where their centers are placed at the maximal contrast-to-tissue ratio of UCA over surrounding tissue. In the design, center points and SD are varied and investigated in order to achieve the best filter for enhancing imaging quality both in terms of contrast and spatial resolution. In general, the frequency response of the QF from the discrete Fourier transform (DFT) can be expressed as (Zhu *et al.*, 1999)

$$H\left(e^{j\omega_{1k}},\ e^{j\omega_{2l}}\right)=\sum_{n_1=0}^{N_1-1}\sum_{n_2=0}^{N_2-1}h\left(n_1,\ n_2\right)\exp\left(-jn_1\omega_{1k}\right)\exp\left(-jn_2\omega_{2l}\right) \tag{1}$$

where $H\left(e^{j\omega_{1k}},\ e^{j\omega_{2l}}\right)$ is a 2D frequency response of the QF, $h(n_1,n_2)$ is the coefficients of the QF, and N_1 and N_2 are the length of the QF on n_1 and n_2, respectively. However, our goal in the design is to calculate coefficients of the QF, $h(n_1,n_2)$, from the frequency response given by

$$H\left(e^{j\omega_{1k}},\ e^{j\omega_{2l}}\right)=G\left(\omega_{1k},\ \omega_{2l}\right)\exp\left(j\phi\left(\omega_{1k},\ \omega_{2l}\right)\right) \tag{2}$$

where $G\left(\omega_{1k},\ \omega_{2l}\right)$ represents the desired magnitude response based on the 2D Gaussian filters and $\phi\left(\omega_{1k},\ \omega_{2l}\right)$ is the phase response, which can be expressed as (Zhu *et al.*, 1997)

$$\phi\left(\omega_{1k},\ \omega_{2l}\right)=-\frac{N_1-1}{2}\omega_{1k}-\frac{N_2-1}{2}\omega_{2l} \tag{3}$$

where $\omega_{1k}=\left(2\pi k/M_1\right)-\pi$, k = 0, 1, ..., M_1-1 and $\omega_{1l}=\left(2\pi l/M_2\right)-\pi$, $l=0, 1, ..., M_2-1$. $(N-1)/2$ is the phase delay of the signal output when $N_1=N_2=N$ is the size of the QF. After we derive the frequency response $H\left(e^{j\omega_{1k}},\ e^{j\omega_{2l}}\right)$ from Equation 2, we can obtain the coefficients $h\left(n_1,\ n_2\right)$ using the inverse discrete Fourier transform (IDFT). The desired magnitude response of the QF based on the 2D Gaussian filters is given by (McAndrew, 2004)

$$G\left(\omega_{1k},\ \omega_{2l}\right)=\frac{G_1\left(\omega_{1k},\ \omega_{2l}\right)+G_2\left(\omega_{1k},\ \omega_{2l}\right)}{\max\left\{G_1,\ G_2\right\}} \tag{4}$$

$$G_i\left(\omega_{1k},\ \omega_{2l}\right)=\exp\left(-\frac{\left(\omega_{1k}-\omega_{ai}\right)^2+\left(\omega_{2l}-\omega_{bi}\right)^2}{2\sigma^2}\right),\ i=1,2 \tag{5}$$

and $G_1\left(\omega_{1k},\ \omega_{2l}\right)$ and $G_2\left(\omega_{1k},\ \omega_{2l}\right)$ represent the 2D Gaussian filters centered at $\left(\omega_{a1},\ \omega_{b1}\right)$ and $\left(\omega_{a2},\ \omega_{b2}\right)$, respectively, and σ is the SD of Gaussian filters. Parameters to be considered for the design are shown in Figure 1. The center of the desired QF are approximately situated at the peaks where the contrast-to-tissue ratio of UCA over surrounding tissue is maximal.

When the linear-phased QF based on the 2D Gaussian filters in the frequency domain is formed, the filter coefficients, $h\left(n_1,\ n_2\right)$, can be obtained using the IDFT as following

$$h\left(n_1,\ n_2\right)=\frac{1}{M_1M_2}\sum_{k=0}^{M_1-1}\sum_{l=0}^{M_2-1}H\left(e^{j\omega_{1k}},\ e^{j\omega_{2l}}\right)e^{jn_1\omega_{1k}}e^{jn_2\omega_{2l}} \tag{6}$$

where $H\left(e^{j\omega_{1k}},\ e^{j\omega_{2l}}\right)=G\left(\omega_{1k},\ \omega_{2l}\right)\exp\left(j\phi\left(\omega_{1k},\ \omega_{2l}\right)\right)$ is the desired frequency response, M_1 and M_2 are the number of points used in IDFT along ω_{1k} and ω_{2l}, respectively. In this paper, we use $M_1=M_2=M=2^n$, n is a positive integer number.

Figure 2 shows a flowchart of the quadratic imaging generation for the design approach. First, we set an initial value for the size of the QF, N, and the number of points used in the DFT and IDFT, M. Next, two parameters, i.e., SD and two center points of the 2D Gaussian filters are chosen

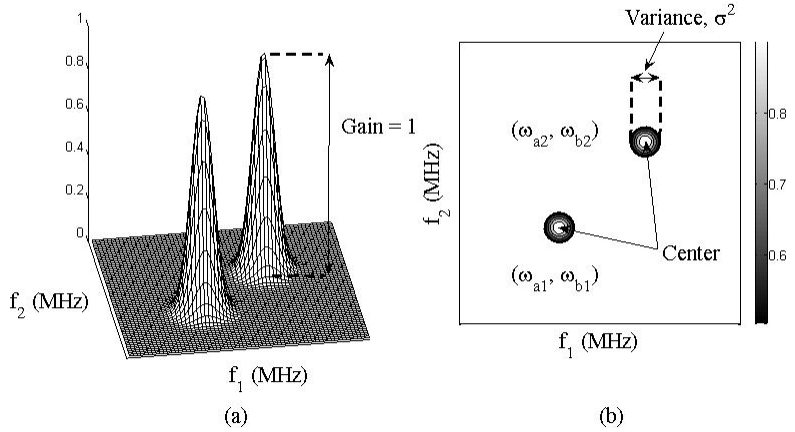

Figure 1. Two parameters in the design of a QF based on a modified 2D Gaussian function in the frequency domain: Variance and center points.

from the regions where the ratio of contrast-to-tissue magnitude is maximal. Then, we form the QF in the frequency domain and take IDFT to obtain the filter coefficients. We measure the difference of the desired QF and the QF from IDFT using normalized mean square error (NMSE), which is given by

$$\text{NMSE} = \frac{\sum\sum\left(|H| - \left|\hat{H}_m\right|\right)^2}{\sum\sum |H|^2} \times 100\% . \qquad (7)$$

If the NMSE is higher than the value that we define (ε), we can increase the kernel size, *N*, in order to reduce the NMSE until we obtain the defined NMSE. The QF based on the 2D Gaussian filters with optimal parameters should enhance the UCA components but suppress the tissue signals. In addition, we use signal outputs from the QF to produce a gray-level image, which provides better quality for medical diagnosis.

3. Materials and Methods

3.1 Experimental setup and data acquisition

The ultrasound data used in this paper are supported by ESAOTE S.p.A, Genoa, Italy. Details of experimental setup and data acquisitions are as follows. The experiment was conducted *in vivo* on a guinea pig. Bolus injections of SonoVue™ (Bracco Research SA, Geneva, Switzerland), a UCA consisting of sulfur hexafluoride gas bubbles coated by a flexible phospholipidic shell, were administered with concentration 0.01 mL/kg. Three-cycle pulses at 1.56 MHz were transmitted with mechanical index 0.158 to scan the kidney of the guinea pig. RF data were acquired with 16-bit resolution at 20-MHz sampling frequency. In addition, all RF data were recorded and saved for off-line processing by the Technos MPX ultrasound system (ESAOTE S.p.A, Genoa, Italy) with a convex array probe (CA430E; ESAOTE S.p.A, Genoa, Italy).

3.2 Power spectrum

After data acquisition, we determine the power spectra of RF A-lines from the UCA regions compared with those from the tissue regions. The power spectrum of the A-line data is obtained by using the periodogram method with a weighted sequence. The multiplication of the weighted sequence, i.e. window, in the time domain is convolution in the frequency domain, so some resolution gets lost by smearing and spectral leakage. However, the trend of the signal's estimated power spectral density (PSD) can be enhanced by the use of the window filters with faster decaying side-lobes. The expression used to calculate the power spectrum is given by (Stoica and Moses, 1997)

$$S\left(e^{j\omega}\right) = \frac{\frac{1}{n}\left|\sum_{i=1}^{n} w_i x_i \, e^{-j\omega i}\right|^2}{\frac{1}{n}\sum_{i=1}^{n}|w_i|^2} \qquad (8)$$

where $S\left(e^{j\omega}\right)$ is a power spectrum, $[x_1, \ldots, x_n]$ is a signal sequence, and $[w_1, \ldots, w_n]$ is a weighted sequence. This expression is an estimate of the power spectrum of signal sequence $[x_1, \ldots, x_n]$ weighted by the window sequence $[w_1, \ldots, w_n]$. The periodogram uses an n-point FFT to compute the PSD as $S\left(e^{j\omega}\right)/F$ where F is a sampling frequency. Twenty-one segments of A-lines from the UCA and tissue regions are used to determine the power spectra. Each segment consists of 201 data samples. Hanning window is chosen as the weighted signal sequence in this paper. An n-point symmetric Hanning window can be expressed as

$$w[k+1] = 0.5\left(1 - \cos\left(2\pi \frac{k}{n+1}\right)\right), \; k = 0, \ldots, n-1 \qquad (9)$$

3.3 Contrast resolution

We use a contrast-to-tissue ratio (*CTR*) as a measure-

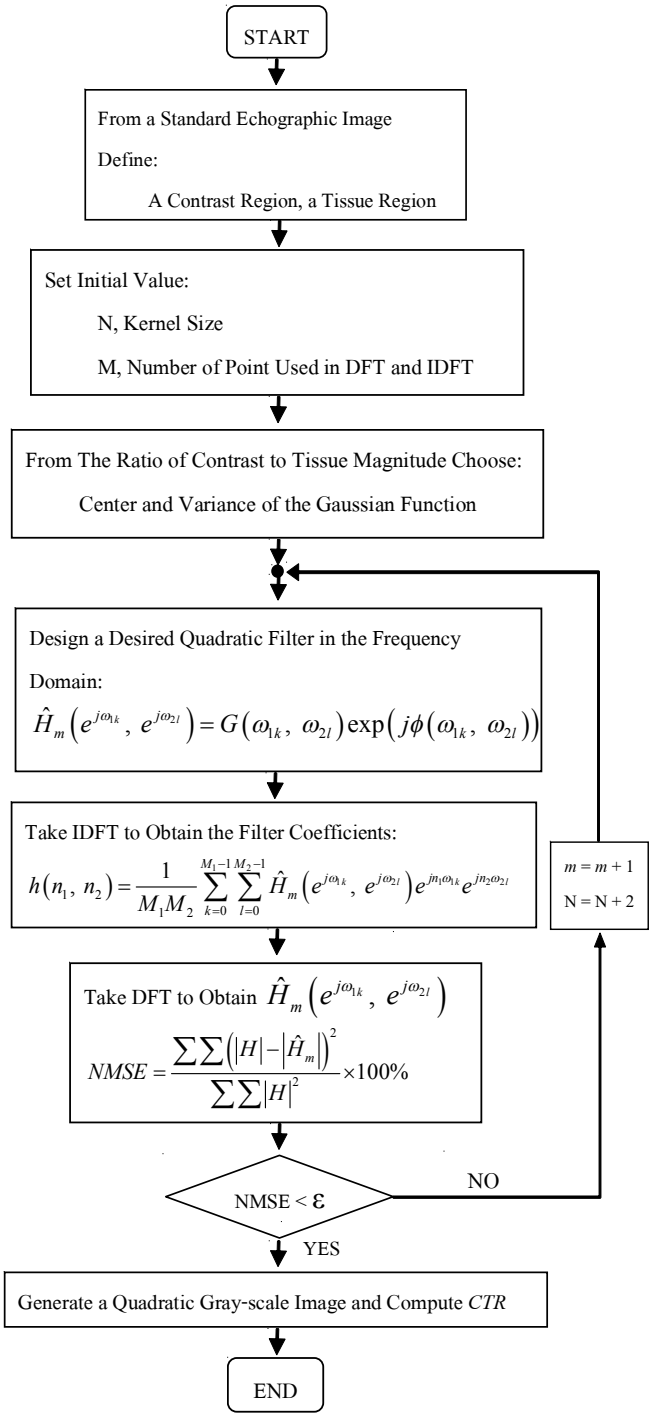

Figure 2. Flowchart of the algorithm for the QF design in the frequency domain.

ment of the QF's capability in extracting the quadratic components. The *CTR* value is calculated from the ratio of the average power of signals in the UCA region to the average power of signals in the tissue region. The appropriate QF for producing a gray-level image with enhanced quality should provide a high *CTR* value. The *CTR* value used to measure contrast resolution of images is given by (Al-Mistarihi *et al.*, 2004a,b)

$$CTR = 10\log_{10}\left(\frac{\bar{P}_C}{\bar{P}_T}\right) \tag{10}$$

where $\bar{P}_C$ and $\bar{P}_T$ are the average power of signals in UCA and tissue regions, respectively. The average power is obtained by

$$\bar{P} = \frac{1}{IJ}\sum_{i=1}^{I}\sum_{j=1}^{J}x_{ij}^2 \tag{11}$$

where x_{ij} is the amplitude of signal in the reference region.

4. Results and Discussion

4.1 Two-dimensional frequency characteristics

The gray image of the kidney is shown in Figure 3(a) with 50 dB dynamic range. The white dotted line in the image indicates the boundary of the kidney. Note that the white dotted line showing the kidney boundary was approximately drawn. The objective is to provide a better understanding to the readers of the kidney image comparisons before and after processing. The UCA and tissue signals are situated inside and outside this boundary, respectively. The reference tissue and UCA regions used to calculate of power spectra are on the left and right white boxes, respectively. The harmonic spectrum of UCA echoes between 2.5 MHz and 4 MHz band are broader than those from the tissue echoes. This result

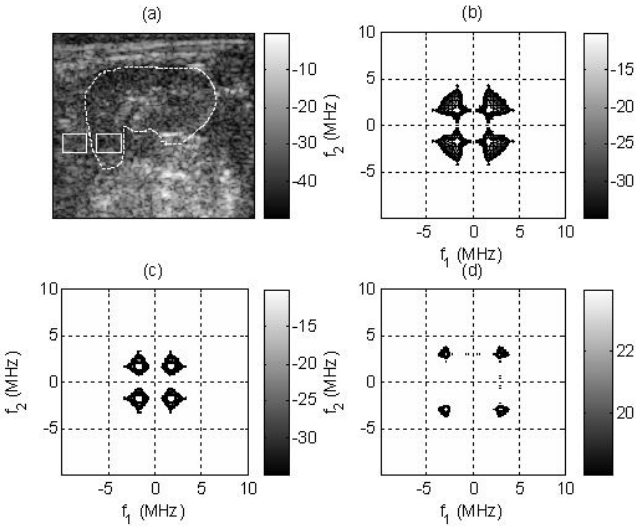

Figure 3. (a) B-mode image of the guinea pig's kidney. (b) Filled contour plot of magnitude 2D frequency response from the UCA region: $\left|X_{CT}\left(e^{j\omega_1}\right)X_{CT}\left(e^{j\omega_2}\right)\right|$ (c) Filled contour plot of magnitude 2D frequency response from tissue region: $\left|X_{TS}\left(e^{j\omega_1}\right)X_{TS}\left(e^{j\omega_2}\right)\right|$. (d) Filled contour plot of the ratio of contrast-to-tissue magnitude: $\left|\frac{X_{CT}\left(e^{j\omega_1}\right)X_{CT}\left(e^{j\omega_2}\right)}{X_{TS}\left(e^{j\omega_1}\right)X_{TS}\left(e^{j\omega_2}\right)}\right|$.

obviously shows the fundamental and second harmonic frequency generation due to UCAs. On the other hand, the signals from tissue regions contain only the transmitted frequency at 1.56 MHz. For more details of the power spectra of UCA ($\left|X_{CT}\left(e^{j\omega}\right)\right|$) and tissue ($\left|X_{TS}\left(e^{j\omega}\right)\right|$) regions please see Phukpattaranont and Chetpattananondh (2005) and Nilmanee *et al.* (2006).

Figure 3(b), (c), and (d) show filled contour plots of the magnitude of the 2D frequency responses in the (ω_1, ω_2) plane. The magnitude 2D frequency responses obtained using RF data in the UCA ($\left|X_{CT}\left(e^{j\omega_1}\right)X_{CT}\left(e^{j\omega_2}\right)\right|$) and tissue ($\left|X_{TS}\left(e^{j\omega_1}\right)X_{TS}\left(e^{j\omega_2}\right)\right|$) regions are shown in Figure 3(b) and (c), respectively. The ratio of contrast to tissue magnitude i.e. $\left|\frac{X_{CT}\left(e^{j\omega_1}\right)X_{CT}\left(e^{j\omega_2}\right)}{X_{TS}\left(e^{j\omega_1}\right)X_{TS}\left(e^{j\omega_2}\right)}\right|$ is shown in Figure 3(d). We can clearly see that there are four distinct regions where UCA is higher than tissue. Consequently, the magnitude 2D frequency response of the desired QF is guided to have the centers around these distinct peaks.

4.2 Center changing

Figure 4 shows the gray-level images of the guinea pig's kidney from signals after filtering with the QF by varying center points. The SD is selected to be 0.34 for all designs in order to investigate the appropriate center points. Images after filtering with the QF produced from the center points (2.90, 2.90) and (-2.90, -2.90) MHz, (3.12, 3.12) and (-3.12, -3.12) MHz, (3.30, 3.30) and (-3.30, -3.30) MHz, (3.70, 3.70) and (-3.70, -3.70) MHz are shown in Figure 4(a), (b), (c), and (d), respectively. The *CTR* values from images in Figure 4(a), (b), and (c) are in the increasing order, i.e., 14.7, 22.1, and 24.8 dB, respectively. When the center points are away from the peak, i.e., (3.70, 3.70) and (-3.70, -3.70) MHz, the *CTR* value of the quadratic image is reduced to be 18.6 dB. It is shown that images in Figure 4(b) and (c) have comparable contrast resolutions and they are better than those from images in Figure 4(a) and (d). The echogenicity of the UCA regions appears brighter than that from surrounding tissue regions. In addition, we can clearly visualize the kidney shape and large vascular structures inside the kidney. However, the spatial resolution of all gray-level images is preserved.

4.3 SD changing

The center points with (3.30, 3.30) MHz and (-3.30, -3.30) MHz are chosen for all designs of SD changing. Figure 5 shows gray-level images of the guinea pig's kidney from signals after filtering with the QF from various SD values. Images after filtering with the QF produced from the SD of 0.20, 0.35, 0.45, and 0.55 are shown in Figure 5(a), (b), (c), and (d), respectively. In addition, the *CTR* values of images in Figure 5(a), (b), (c), and (d) are 24.7, 24.5, 20.6, and 14.2 dB,

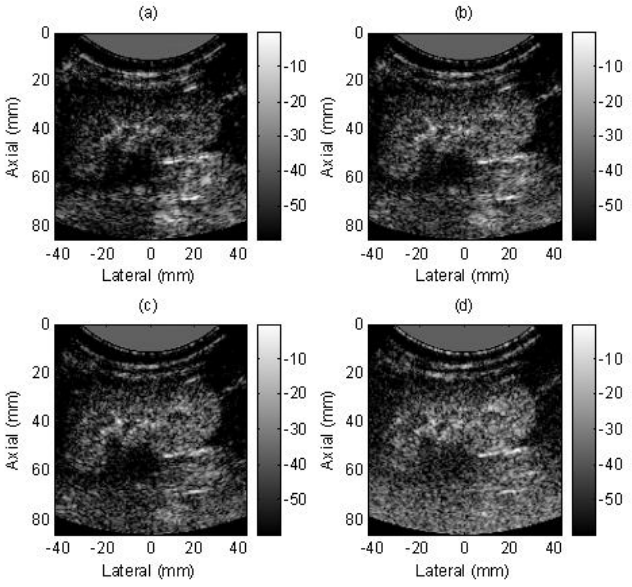

Figure 4. Gray-level images of the guinea pig's kidney from signals after filtering with the QF by varying center points (a) (2.90, 2.90) and (-2.90, -2.90) MHz (b) (3.12, 3.12) and (-3.12, -3.12) MHz (c) (3.30, 3.30) and (-3.30, -3.30) MHz (d) (3.70, 3.70) and (-3.70, -3.70). SD is fixed at 0.34.

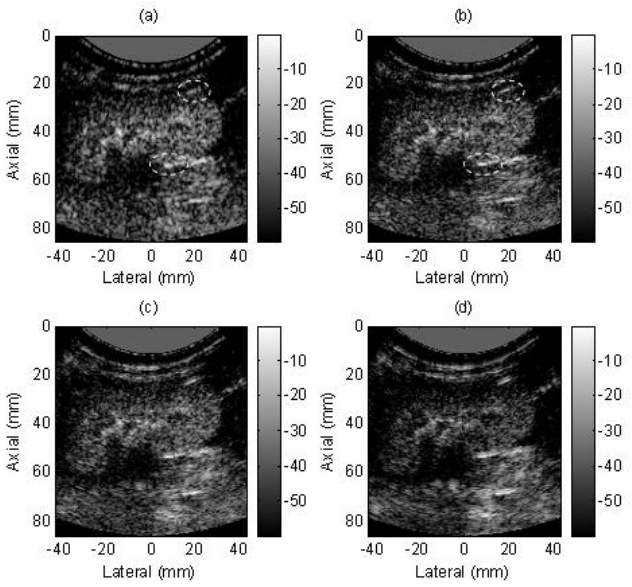

Figure 5. Gray-level images of the guinea pig's kidney from signals after filtering with the QF by varying SD to be (a) 0.20, (b) 0.35, (c) 0.45, and (d) 0.55. Center points are fixed to (3.30, 3.30) and (-3.30, -3.30) MHz. The reflections in the white circles indicate the loss of spatial resolution of the image in (a) compared to that in (b).

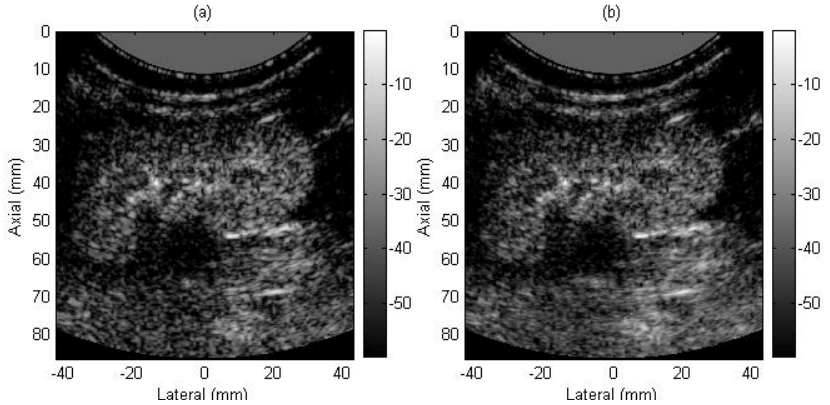

Figure 6. Quadratic images of the pig's kidney produced from the QF design based on: (a) The 2D modified Gaussian filter with center (3.30, 3.30), (-3.30, -3.30) MHz, and SD 0.34. (b) The linear plus quadratic prediction model.

respectively. These are in agreement with visualized inspection. It can be seen that the QF with SD from 0.20 and 0.35 are comparable in terms of contrast resolution, i.e., *CTR*. However, the QF with SD 0.35 provides better spatial resolution compared to the QF with SD 0.20. The loss of spatial resolution of the image in Figure 5(a) can be noticed from the reflections in the white circles, which appear thicker compared to those in Figure 5(b).

4.4 Comparison of quadratic images from two different design methods

Quadratic images of pig's kidney produced using two different approaches, i.e., the 2D Gaussian filter with centers at (3.30, 3.30) and (-3.30, -3.30) MHz, SD 0.34 and the linear plus quadratic prediction model, are shown in Figure 6(a) and (b), respectively. One can see that both of them are comparable in terms of spatial resolution. However, the image produced from output signals of the new design is slightly superior to that from the time domain method in terms of contrast resolution, i.e., *CTR* value of 24.8 dB compared to 22.0 dB.

5. Conclusions

We propose a novel design method of quadratic filters for contrast-assisted ultrasonic imaging in the frequency domain. The design approach is based on the IDFT of the sum of two 2D Gaussian filters centered in the position where the contrast-to-tissue magnitude is maximal. Performance of the QF from the new design is evaluated using *in vivo* ultrasound data. Results show that quadratic images produced using the QF with center points at (3.30, 3.30) and (-3.30, -3.30) MHz, SD 0.34 is better than those from the QF based on a linear plus quadratic prediction model in terms of contrast resolution. In addition, both of them are comparable in terms of spatial resolution.

The new proposed technique provides easy and efficient tools for designing the QF for contrast-assisted ultrasonic imaging. The method can be easily applied to any other contrast-assisted images. The image quality after processing depends on the appropriate selection of centers and SDs of the two 2D Gaussian filters. These parameters can be estimated based on the ratio of contrast-to-tissue magnitude of new images. Moreover, the design of quadratic filters providing a better performance of the image quality for medical diagnosis is possible with this new method and it is subject of ongoing research.

Acknowledgement

In addition, this research project was funded by a grant from the Faculty of Engineering, Prince of Songkla University through Contract No. Eng-51-2-7-02-0004-S. The authors thank ESAOTE S.p.A, Genoa, Italy for supporting the *in vivo* data used in this paper.

References

Al-Mistarihi, M.F., Phukpattaranont, P. and Ebbini, E.S. 2004a. A two-step procedure for optimization of contrast sensitivity and specificity of post-beamforming Volterra filters. Proceedings of the 2004 the Institute of Electrical and Electronics Engineers International Ultrasonics Symposium, Montreal, Canada, August 23-27, 2004, 978-981.

Al-Mistarihi, M.F., Phukpattaranont, P. and Ebbini, E.S. 2004b. Post-beamforming third-order Volterra filter (ThOVF) for pulse-echo ultrasonic imaging. Proceedings of 2004 the Institute of Electrical and Electronics Engineers International Conference on Acoustics, Speech, and Signal Processing, Montreal, Canada, May 17-21, 2004, 97-100.

Cosgrove, D. 2006. Ultrasound contrast agents: An overview. European Journal of Radiology. 60, 324-330.

De Jong, N., Cornet, R., and Lancee, C.T. 1994a. Higher harmonics of vibrating gas filled microspheres. Part one: Simulations. Ultrasonics. 32(6), 447-453.

De Jong, N., Cornet, R., and Lancee, C.T. 1994b. Higher harmonics of vibrating gas filled microspheres. Part two: Measurements. Ultrasonics. 32(6), 455-459.

Feinstein, S.B., Shah, P.M., Bing, R.J., Meerbaum, S., Corday, E., Chang, B.L., and Santillan, G., and Fujibayashi, Y. 1984. Microbubble dynamics visualized in the intact capillary circulation. Journal of the American College of Cardiology. 4, 595-600.

Frinking, P.J.A., Bouakaz, A., Kirkhorn, J., Ten Cate, F.J., and de Jong, N. 2000. Ultrasound contrast imaging: current and new potential methods. Ultrasound in Medicine & Biology. 26(6), 965-975.

Frischke, C., Lindner, J.R., Wei, K., Goodman, N.C., Skyba, D.M., and Kaul, S. 1997. Myocardial perfusion imaging in the setting of coronary artery stenosis and acute myocardial infarction using venous injection of a second-generation echocardiographic contrast agent. Circulation. 96(3), 959-967.

McAndrew, A. 2004. Introduction to digital image processing with MATLAB. Thomson Course Technology, U.S.A., 101-104.

Nilmanee, T., Phukpattaranont P., and Jindapetch, N. and Thienmontri, S. 2006. Frequency characteristic of pulse-echo signals from contrast-assisted ultrasound, The 29th Electrical Engineering Conference, Pattaya, Thailand, November 9-10, 2006, 949-952.

Phukpattaranont, P. and Ebbini, E.S. 2003. Post-beamforming second-order Volterra filter for pulse-echo ultrasonic imaging. The Institute of Electrical and Electronics Engineers Transactions on Ultrasonics, Ferroelectrics and Frequency Control. 50(8), 987-1001.

Phukpattaranont, P., and Chetpattananondh, K. 2005. Post-beamforming second-order Volterra filters for contrast agent imaging: A frequency-domain aspect. Proceedings of the 26th Symposium on Ultrasonic Electronics, Yokohama, Japan, November 16-18, 2005, 281-282.

Ramnarine, K.V., Kyriakopoulou, K., Gordon, P., McDicken, N.W., McArdle, C.S. and Leen, E. 2000. Improved characterization of focal liver tumours: Dynamic power doppler imaging using NC100100 echo-enhancer. European Journal of Ultrasound. 11(2), 95-104.

Stoica, P. and Moses, R. 1997. Introduction to spectral analysis. Upper Saddle River, NJ: Prentice Hall, p. 15.

Tanaka, S., Kitamra, T., Yoshioka, F., Kitamura, S., Yamamoto, K., Ooura, Y. and Imaoka, T. 1995. Effectiveness of galactose based intravenous contrast medium on color Doppler sonography of deeply located hepatocellular carcinoma. Ultrasound in Medicine & Biology. 21(2), 157-160.

Zhu, W.P., Ahmad, M.O. and Swamy, M.N.S. 1997. A Least-Square Method for the Design of 2-D FIR Digital Filters with Arbitrary Frequency Responses. Proceedings of the Institute of Electrical and Electronics Engineers International Symposium on Circuits and Systems. June, 1997, 769-772.

Zhu, W.P., Ahmad, M.O. and Swamy, M.N.S. 1999. A Least-Square Design Approach for 2-D FIR Filters with Arbitrary Frequency Response. The Institute of Electrical and Electronics Engineers Transactions on Circuits and Systems Part II. 46(8), 1027-1034.